EMTDC Assessment of a New Type of VSC for Back to Back HVdc Interconnections

Liu Yonghe, J. Arrillaga, and N.R.Watson

Dept. of Electrical and Computer Engineering, University of Canterbury, Christchurch, New Zealand (e-mail: yli35@student.canterbury.ac.nz, j.arrillaga@elec.canterbury.ac.nz and n.watson@elec.canterbury.ac.nz),

***Abstract* – A new type of voltage source converter is described based on the reinjection of dc. voltage pulses into the main series connected bridges via the d.c side neutral point. This configuration produces a 36-pulse voltage waveform at the converter side of the interface transformers. The paper analyses the steady state and dynamic performance of the scheme when applied to a back to back HVdc interconnection.**

Keywords – HVdc, Voltage Source Converter, dynamic assessment

I. INTRODUCTION

Given the large power and voltage ratings involved, the HVdc technology has until recently been entirely dependent on line-commutated current source conversion using thyristors. The latter, however, are likely to face growing competition from schemes based on turn off devices and voltage source conversion [1][2][3].

Moreover, the high switching rates needed to provide acceptable voltage and current waveforms has encouraged the development of new converter configurations, with the purpose of limiting the use of pulse width modulation(PWM). In particular, a variety of multi-level schemes have been proposed to control the low order characteristic harmonics, while still relying on PWM for the control of the higher orders.

A recent publication [4] has described a new principle of voltage source conversion based on the addition of d.c. voltage pulses to the converter a.c. voltage waveform and applied it to the 12-pulse parallel configuration. This concept is extended in this paper to the series converter configuration used by the HVdc interconnections. In this case the d.c. voltage pulses, reinjected to the converters via the d.c. side neutral point, shape the conventional rectangular phase voltage into a 36-step waveform. The description that follows includes the steady state and dynamic performance of the proposed configuration.

II. SYSTEM DESCRIPTION IN THE STEADY STATE

Figure 1 shows the proposed back-to-back configuration, which consists of two equal VSC units. The description, therefore, is made with reference to one of them only. A reinjection bridge is connected across the d.c. capacitor and the output voltage waveform of the reinjection bridge consists of dc voltage pulses at six times the fundamental frequency. The magnitude of these pulses is adjusted by the reinjection transformer ratio to the level required to minimise the harmonic content of the output voltage waveform. Finally, the d.c. voltage pulses, injected into the main converter via the dc side neutral point are added to the individual valves voltage waveforms.

To simplify the description the converter system is assumed to consist of ideal switches and transformers and contain unlimited capacitance on the dc side. The turn ratios of the converter transformers in the 12-pulse configuration ensure that the voltages across the upper (U_{CY}) and lower ($U_{C.}$) bridges are the same (U_C).

Therefore the voltages across the Y/Y and Y/. connected bridges are determined by the capacitor voltage (U_{CY} and $U_{C.}$) and the reinjection voltage (u_j), i.e.

$$v_Y = U_{CY} - u_j \tag{1}$$

$$v_. = U_C + u_j \tag{2}$$

The reinjection voltage shapes the ac output voltage waveforms of both bridges simultaneously. Three levels of u_j are produced, i.e. zero voltage (by turning off the reinjection bridge), $k_j\left(U_{C.} + U_{CY}\right)$ and $-k_j\left(U_{C.} + U_{CY}\right)$ (by forward and reverse connection of the reinjection bridge to

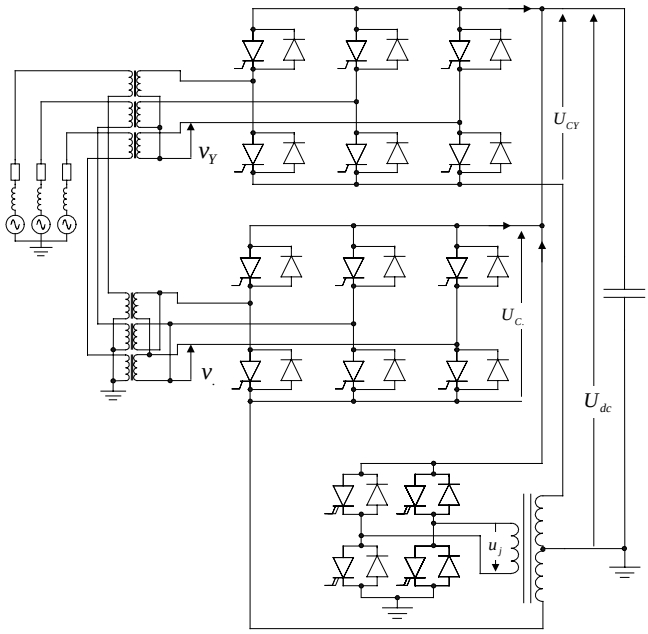

Fig. 1 Reinjection Voltage Source Converter

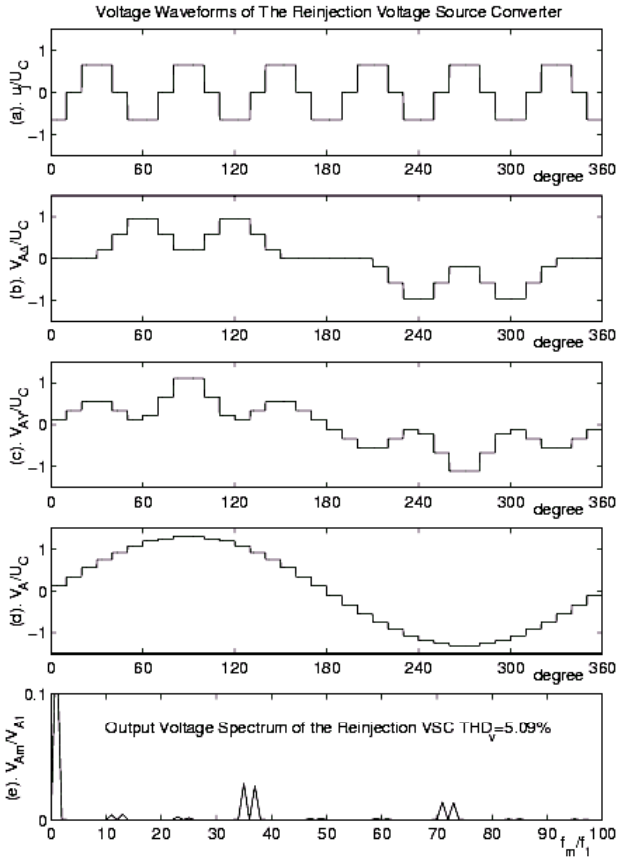

Fig. 2 Voltage Waveforms of the Reinjection VSC

the capacitor respectively; k_j being the proportion of dc voltage reinjected). The three level combination changes every 30 degrees, requiring another 30 degrees to return to the original state. Thus the reinjection voltage u_j is a pulse train of six times the fundamental frequency.

The above switching pattern produces an 18-pulse voltage waveform on the primary side of each of the series connected converter transformers and therefore a 36-pulse waveform on the a.c. system side of the voltage source converter.

III. Output Voltage Waveforms

Figure 2 shows the voltage waveform development across the voltage source converters of the back to back interconnection. All the magnitudes are in per unit with reference to the d.c. voltage U_{dc}. The reinjection voltage, shown in Figure 2(a), is added to the voltage waveforms of the star and delta connected bridges in Figures 2(b) and 2(c) respectively. These two waveforms are then combined on the primary side of the converter transformers windings (which are connected in series) yielding the output voltage waveform shown in Figure 2(d). A detail analysis of the voltage waveform is given in the appendix.

Finally Figure 2(e) displays the harmonic spectrum of the output voltage waveform, which clearly shows the 36 pulse nature of the proposed configuration.

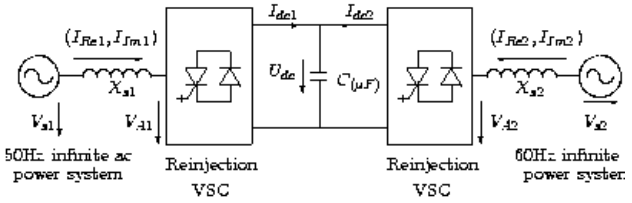

Fig 3 BTB VSC Link System

VI. Dynamic Equivalent

Unlike PWM, where the voltage amplitude and phase angle control is made independently, the reinjection dual converter system has no independent voltage amplitude and phase angle freedom, due to the fundamental frequency switching conditions. The input control parameters of the dual converters are the phase angle differences between the converter output voltages and their respective source voltages. The output parameters are the active power transfer, the reactive power generation and the dc side voltage, although in the control implementation the use of active and reactive current components is preferred to their respective powers.

The dynamic model of the dual converter system is described with reference to the simplified equivalent circuit shown in Figure 3 which represents a BTB link interconnecting systems of nominal frequencies of 50 and 60 Hz. Under perfectly balanced operation the interface transformers are represented by their fundamental leakage reactances X_{s1} and X_{s2}. Through these two reactors the dual converter system is connected to two infinite power systems, represented by ideal voltage sources V_{s1} and V_{s2}. The dual converter ac output voltages are V_{A1} and V_{A2}, while ϕ_1 and ϕ_2 are the phase angles relative to their respective system voltage sources. The ac output currents are specified by their real and imaginary components i.e. ($I_{\mathrm{Re}1}, I_{\mathrm{Im}1}$) and ($I_{\mathrm{Re}2}, I_{\mathrm{Im}2}$). Finally the dc output currents are I_{dc1} and I_{dc2}, and the common shared capacitor voltage is denoted as U_{dc}.

Using the above terminology the following formulas can be written:

$$P_1 = \frac{3V_{s1}V_{A1}}{X_{s1}}\sin(\phi_1) \tag{3}$$

$$P_2 = \frac{3V_{s2}V_{A2}}{X_{s2}}\sin(\phi_2) \tag{4}$$

$$I_{\mathrm{Re}1} = \frac{V_{A1}}{X_{s1}}\sin(\phi_1) \tag{5}$$

$$I_{\mathrm{Re}2} = \frac{V_{A2}}{X_{s2}}\sin(\phi_2) \tag{6}$$

$$I_{dc1} = \left[P_1 - P_{L1}\right]/U_{dc} \tag{7}$$

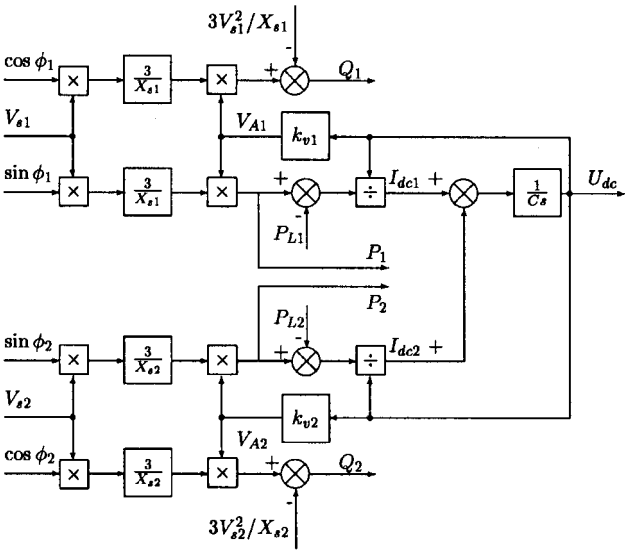

Fig. 4 System Control Block Diagram

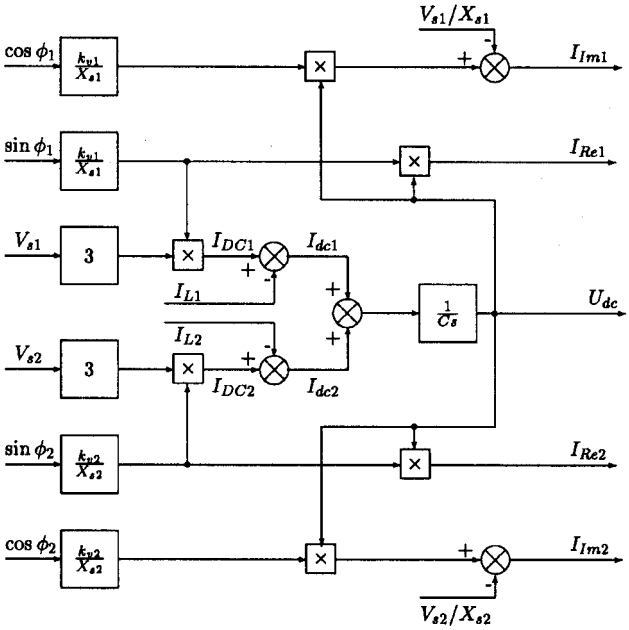

Fig. 5 Modified Control Block Diagram

$$I_{dc2} = \left[P_2 - P_{L2}\right]/U_{dc} \tag{8}$$

$$Q_1 = \frac{3V_{s1}V_{A1}}{X_{s1}}\cos(\phi_1) - \frac{3V_{s1}^2}{X_{s1}} \tag{9}$$

$$Q_2 = \frac{3V_{s2}V_{A2}}{X_{s2}}\cos(\phi_1) - \frac{3V_{s2}^2}{X_{s2}} \tag{10}$$

$$I_{\mathrm{Im}1} = \frac{V_{A1}}{X_{s1}}\cos(\phi_1) - \frac{V_{s1}}{X_{s1}} \tag{11}$$

$$I_{\mathrm{Im}2} = \frac{V_{A2}}{X_{s2}}\cos(\phi_2) - \frac{V_{s2}}{X_{s2}} \tag{12}$$

$$U_{dc} = \frac{1}{C}\int \left(I_{dc1} + I_{dc2}\right)dt \tag{13}$$

where P_1 and P_2 are the real powers transfers at the 50Hz and the 60Hz power systems, P_{L1} and P_{L2} are the losses of the two reinjection converters, and Q_1 and Q_2 are the reactive powers generated by the two reinjection converters.

A. The Dual VSC System Control Model

From equations 3 to 13 and the relationships $V_{A1} = k_{v1}U_{dc}$ and $V_{A2} = k_{v2}U_{dc}$, the block diagram of the BTB reinjection VSC link needed to control the active and reactive powers is illustrated in Figure 4.

Using the following power-current relationships

$$I_{DC1} = P_1/U_{dc} = \left[\left(k_{v1}/X_{s1}\right)\sin(\phi_1)\right]\left(3V_{s1}\right) \tag{14}$$

$$I_{DC2} = P_2/U_{dc} = \left[\left(k_{v2}/X_{s2}\right)\sin(\phi_2)\right]\left(3V_{s2}\right) \tag{15}$$

and $I_{L1} = P_{L1}/U_{dc}$, $I_{L2} = P_{L2}/U_{dc}$, the control block diagram can be simplified to that of Figure 5, which can be applied directly to control the active and reactive current components.

B. Switching Instants Derivation

As already explained, the main object of the control system is to transfer specified real power and generate the required reactive power. Under normal operating conditions the real and imaginary components of the converter output currents

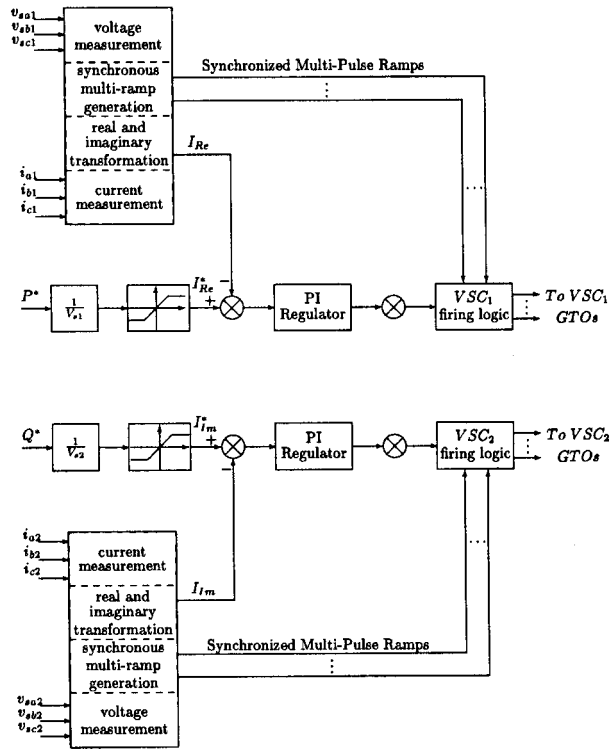

Fig. 6 Control Structure

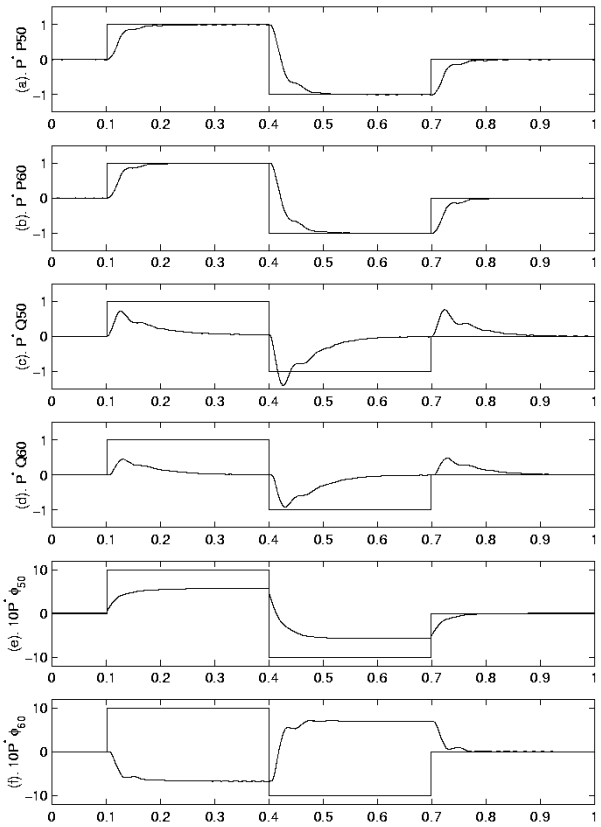

Fig. 7 Real and Imaginary power Dynamic Response

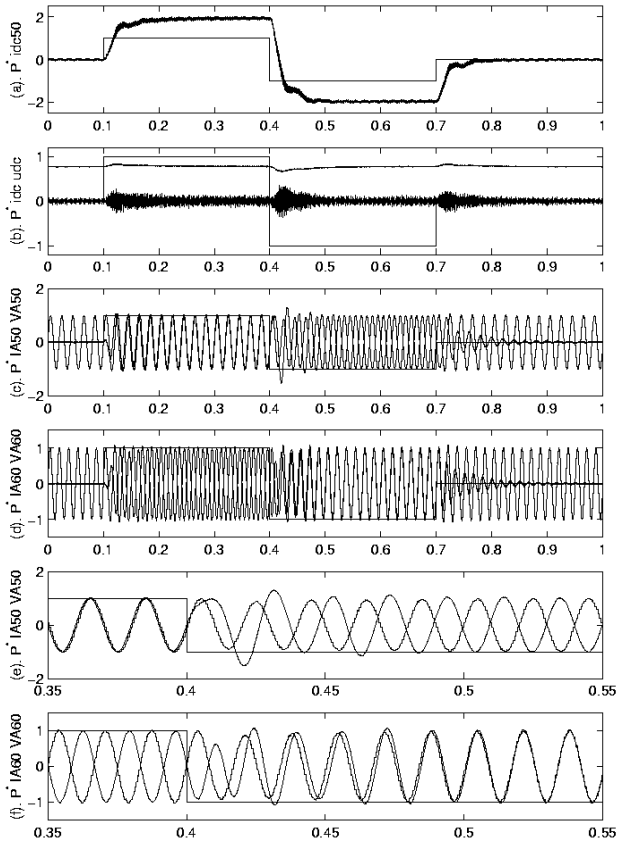

Fig.8 Voltage and Current Response under Real Current Order

directly determine the active and the reactive power, and are, thus, used by the control system instead of the active and reactive powers. Under abnormal conditions a direct control of the real and imaginary current components provides safer system control than one based on the active and reactive powers. The real and imaginary components of the output current on one side converter are related to those on the other side. Therefore the output current real component of the 50Hz source side and the output current imaginary component of the 60Hz source side are set as the control objects, while the imaginary component of the former and the real component of the latter are made dependent on the operation state.

The resulting control structure of the dual converter system is shown in Figure 6. The measured output currents are transformed into their real and imaginary current components, with the source voltages used as references. The multi-pulse ramp signals required by the converter GTO firing logic are synchronized with their respective source voltages. The real and reactive power references P^* and Q^*, are divided by the source voltages to derive the real and imaginary current command. Proportional regulator saturation limitations ensure that the input references of the direct current control system are in the safe operation region, both, under normal source voltages and depressed source voltage conditions. The PI controllers generate the phase angle displacement commands depending on the real and imaginary current errors for the two converters respectively.

V. Dynamic Performance

The test system consists of a 100kV, 100MW, 50/60 Hz BTB interconnector capable of providing ±50 MVAr at each side of the link under normal operating conditions.

The strategy is to control separately the constant real current and imaginary current of the dual converters as depicted in Figure 3. Figures 7 and 8 illustrate the dual converter system dynamic response when subjected to a step change of real current order, while the imaginary current order is kept at zero. Initially the dual converter system operates under no real power interchange and no imaginary current generation. At *t*=100 ms the real current control order is set to 1 pu, that corresponds to 100 MW real power transfer from the 50Hz to the 60Hz system. The real current control order is reversed to -1 pu at *t*=400 ms, and then to zero at *t*=700 ms.

The plots in Figure 7 show the dynamic behavior of the real and imaginary powers of the two asynchronous systems (P_{50} , Q_{50} , P_{60} , Q_{60}) and the two phase angle displacements between the sources and the converter output voltages (ϕ_{50} , ϕ_{60}); the total modelling time is 1000ms.

The plots in Figure 8 show the following voltage and current waveforms:

i_{dc50} (the dc output current of the 50Hz system side converter)

U_{dc} (the dc voltage across the dc capacitor)

i_{dc} (the current through the dc capacitor)

I_{A50} (the phase current of the 50Hz system)

V_{A50} (the phase output voltage of the 50Hz system side converter)

I_{A60} (the phase current of the 60Hz system)

V_{A60} (the phase output voltage of the 60Hz system side converter)

To clarify the dynamic process the waveforms of (I_{A50},V_{A50}) and (I_{A60},V_{A60}) are plotted in greater detail in graphs (e) and (f) for the interval $0.35<t<0.55$. All the waveforms indicate that following the change of the real current order for about 100ms, the system can reach new steady state conditions. In particular graphs (e) and (f) show clearly that in about 3 to 4 cycles the dual converter system output currents and voltages complete the power transfer reversal process with no significant over current. Moreover the voltage and current waveforms clearly show that the harmonic distortion is well under control.

Figures 9 and 10 illustrate the dynamic performance of the dual converter system under zero real current and ±0.5 pu imaginary current orders. The plots in Figures 9 and 10 are arranged as those in Figures 7 and 8

VI. CONCLUSIONS

A new concept of multi-level voltage sourced conversion has been described that produces a 36-step voltage waveform at the converter terminals. Following the theoretical illustration of the ideal steady state waveforms the paper has covered the characteristics of the multi-variable control, coupling and non-linearity. The dynamic performance has been investigated with the help of the PSCAD/EMTDC package.

As the reinjection current shapes the current of the dc capacitor into a high frequency and small amplitude waveform, a smaller size of the dc capacitor can be used, and faster response is obtained during the dynamic process, compared with the conventional converter schemes.

Based on the control function and structure proposed, the dual converter system can respond quickly to track the operating condition order with satisfactory dynamic and steady state characteristics.

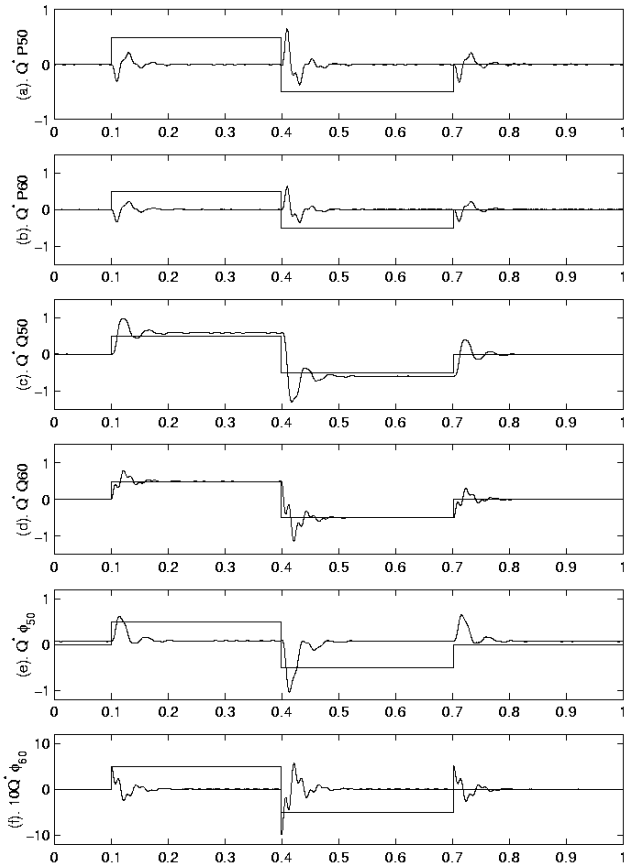

Fig. 9 Real and Reactive Power Response of Imaginary Current order

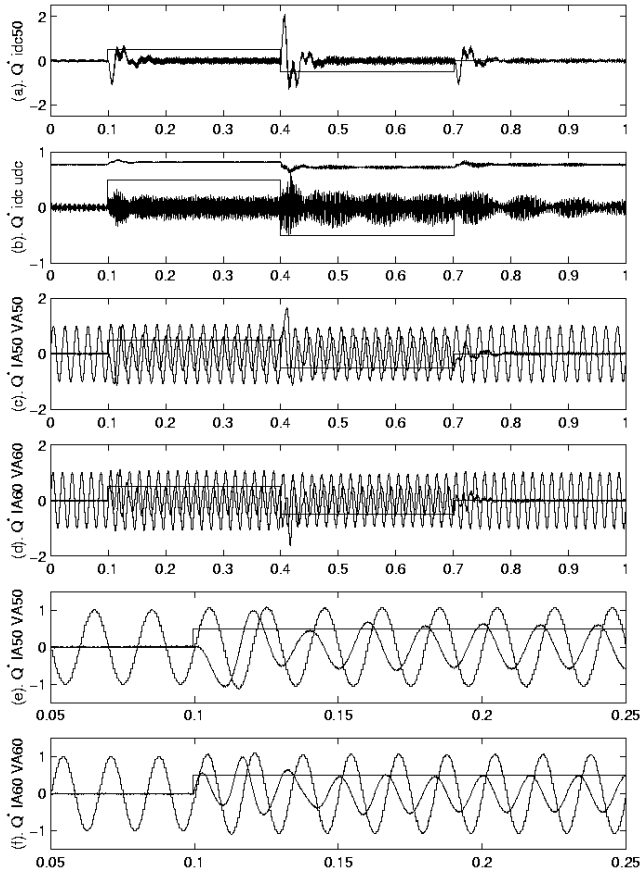

Figure 10. Voltage and Current Response under Imaginary Current Order

REFERENCES

[1] A. Nabae, I. Takahashi and H. Akagi, "A new neutral-point-clamped PWM inverter," IEEE Trans. on Industry Application, Vol. IA-17 (5), pp. 518-523, 1981.

[2] T. Meynard and H. Foch, "Imbricated cells multi-level voltage source inverters for high voltage applications," European power Electronics Journal, Vol. 3 (2), pp. 99-106, 1993.

[3] Song, Yong-Hua. Johns, A. T. (Allan T.), "Flexible A.C. transmission systems (FACTS)," London : Institution of Electrical Engineers, 1999.

[4] Y.H. Liu, J. Arrillaga and N.R. Watson, "Multi-level Voltage Sourced Conversion by Voltage Reinjection at Six times the Fundamental Frequency", Proc. IEE-Electr. Power & Appl., Vol. 149(3), 2002, pp. 201-206